2606
doi:10.1017/S1431927622009904
Microsc. Microanal. 28 (Suppl 1), 2022

Imaging Structural Defects and Associated Oxygen Positions in Li-rich $Li_{1.2}Ni_{0.13}Mn_{0.54}Co_{0.13}O_2$

Weixin Song[1,2,3*], John Joseph Marie[1,2,3], Robert A. House[1,2,3], Peter G. Bruce[1,2,3] and Peter D. Nellist[1,2,3]

[1.] Department of Materials, University of Oxford, Oxford, UK.
[2.] The Faraday Institution, Didcot, UK.
[3.] The Henry Royce Institute, Oxford, UK.
* Corresponding author: weixin.song@materials.ox.ac.uk

Li-rich $Li_{1.2}Ni_{0.13}Mn_{0.54}Co_{0.13}O_2$ has delivered a high specific capacity over 250 mAh g^{-1} as a cathode material in Li-ion batteries compared with conventional layered metal oxides (< 200 mAh g^{-1}). Such high capacity results from the redox reaction of the lattice O^{2-} ions and transition metals (TMs). Despite the boost in the capacities, $Li_{1.2}Ni_{0.13}Mn_{0.54}Co_{0.13}O_2$ still suffers from voltage hysteresis and degradation in the voltage and capacity over cycling [1]. Synthesis efforts aim to overcome these issues. The challenge is $Li_{1.2}Ni_{0.13}Mn_{0.54}Co_{0.13}O_2$ has rather inhomogeneous crystalline structures whose role in affecting the materials performance is unclear [2]. The as-prepared $Li_{1.2}Ni_{0.13}Mn_{0.54}Co_{0.13}O_2$ material contains a number of defects, such as stacking faults, and has raised debates on whether the material is a coherent mixture of *C2/m* Li_2MnO_3 and *R-3m* $LiTMO_2$ phase or a solid solution with the monoclinic phase [2]. The lack of understandings on the pristine structure of $Li_{1.2}Ni_{0.13}Mn_{0.54}Co_{0.13}O_2$ impedes the approach development for new materials.

In this work, we performed simultaneous annular dark field (ADF) imaging and electron ptychography on pristine $Li_{1.2}Ni_{0.13}Mn_{0.54}Co_{0.13}O_2$ prepared by sol-gel method. **Figure 1a** shows the ADF image projected along the pseudo [100] zone axis, which rather than showing only monoclinic [100] projection domains, shows three types of monoclinic domains projected along the [100], [110] and [1-10] zone axis, respectively. The domain variants are due to the faulted stacking of the TM layers in *c* direction. TM layers composing the three types of domains have an in-plane rotation angle of 120 degree with respect to each other and the resulting stacking faults are referred to as rotation type. In the TM layers, Li^+/Ni^{2+} and Co^{3+}/Mn^{4+} cation ordering in a honeycomb pattern leads to the dumbbell contrast in ADF imaging that arising from the mixing Co/Mn atom columns [1]. The dumbbell contrast is not uniformly seen as shown in **Figure 1b**, where cation disordering contrast is seen in the transition regions (labelled with white dash) between the [110] and [1-10] projection domains. **Figure 1c** displays several types of TM layers that lead to cation ordering (O), mixing ordering/disordering (O/D) and disordering (D) contrast in ADF imaging. In addition to the rotation-type stacking faults, **Figure 1d** shows another type resulting from out-of-plane TM layer shift by a vector of *c*/2 in *c* direction, namely shift type. Both types of stacking faults rely on the imaging of TM layers whilst lack the understandings of oxygen stacking. To probe the oxygen lattice, we carried out focused-probe electron ptychography to reconstruct the phase image of the material and use the simultaneous aberration-corrected ADF image to point out TMs. **Figures 2(a-c)** show the simultaneous ADF and ptychographic image and their composite image, respectively, of a rotation-type stacking fault region and **Figures 2(d-f)** show that of a shift-type region. Although TM layers possess a number of rotation-type stacking faults, the oxygen layers are seen in an O3-type stacking, coordinating with the octahedral-site TMs. Such TM-O coordination and the more covalent bonding of TM-O than Li-O lead to O layer mismatch in the shift-type stacking faults,

indicated by the solid and dash circles in Figure 2f. The imaging on the TMs and O layer stacking shows different structure defects in $Li_{1.2}Ni_{0.13}Mn_{0.54}Co_{0.13}O_2$ that can affect materials performance [3].

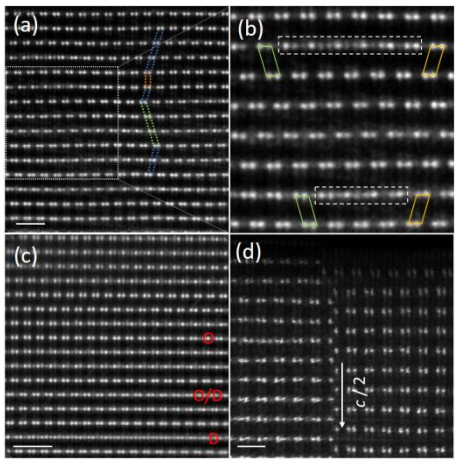

Figure 1. Stacking faults of $Li_{1.2}Ni_{0.13}Mn_{0.54}Co_{0.13}O_2$. (a) ADF image along pseudo [100] zone axis in a rotation-type stacking fault region. White rectangular region is magnified in (b). The red, green and orange tetragons indicate monoclinic domains projected along [100], [110] and [1-10] zone axis, respectively. (c) ADF image of TMs layers showing cation ordering (O), mixed ordering/disordering (O/D) and disordering (D) contrast. (d) ADF image of shift-type stacking fault. Scale bar is 1 nm.

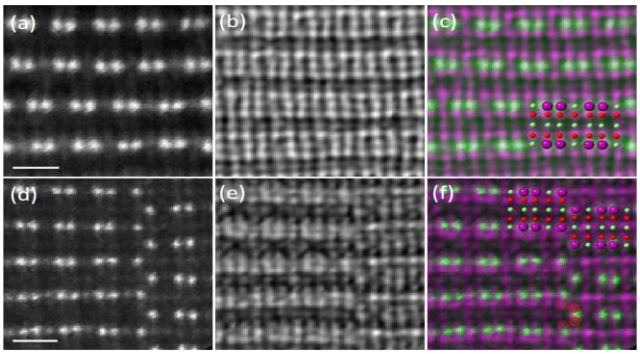

Figure 2. TM and O layer stacking. Faulted region of (a-c) rotation type and (d-f) shift type. (a, d) ADF image. (b, e) Ptychographic image. (c, f) Composite image of the ADF and ptychographic image. Superposed in c and f is the crystal model. Purple sphere is TM, green Li and red O. Scale bar is 0.5 nm.

Reference:

[1] RA House et al., Nat. Energy **5** (2020), p. 777.
[2] AK Shukla et al., Energ. Environ. Sci. **11** (2018), p. 830.
[3] The authors acknowledge use of characterization facilities within the David Cockayne Centre for Electron Microscopy, Department of Materials, University of Oxford and the Faraday Institution (FIRG007, FIRG008), the EPSRC (EP/K040375/1 “South of England Analytical Electron Microscope”) and additional instrument provision from the Henry Royce Institute (Grant reference EP/R010145/1).

https://doi.org/10.1017/S1431927622009904 Published online by Cambridge University Press